Definition and solidity of gold and platinum jewels produced using Selective Laser Melting SLM™ technology

Authors:
Damiano Zito, Alessio Carlotto, Alessandro Loggi, Dr. Patrizio Sbornicchia, Damiano Bruttomesso, Stefano Rappo

Progold S.p.A
Trissino (VI), Italy

Abstract:

In the world of direct additive manufacturing, Selective Laser Melting (SLM™) of powdered metal is currently one of the most attractive new technologies with potential to replace lost-wax investment casting because it enables the production of items with high geometrical complexity which are light and customizable. In addition, it provides several environmental advantages.

In previous testing, improving the quality of items was achieved both by selecting best construction parameters and by developing alloys with greater laser absorption. In this work the dimensional accuracy of actual jewelry items is assessed and the possibility of making lighter items while maintaining adequate structural strength is explored. In addition, the best working parameters for red-gold and platinum alloys were studied. Dimensional accuracy was assessed by building a metal structure and an actual pavé ring.

Then the geometrical conformity of the SLM ring was compared to the original design. The roughness of the metal section, metal density, metal homogeneity, accuracy of ornamental details and quality as a function of orientation on

the build platform will be reported.

Introduction:

In our previous work we studied the production of precious alloy items through an optimization of selective laser melting (SLM). We built elementary units, named vectors, seeking for to obtain the same quality level of simple investment cast shapes. We achieved a high quality level for gold alloys with the use of parallel laser scanning and selecting the optimum set of laser parameters, to avoid the well known formation of surface swelling defects. The adverse effect of some additions (Ga) that leads the formation of this defect was evidenced.

Moreover, we evaluated the effect of support system structure of the items, namely support shape, density and slope angle of walls. The effect of some elements favoring the absorption of laser radiation (Ge, Pt) was underlined. These elements enabled to reduce surface swelling, ejection of metal particles and roughness of the specimens.

In the present work we evaluated the aesthetical and geometrical effects of ornamental details and the mechanical strength of some very light pieces with intricate shape, produced through SLM. Our target was to achieve the flexibility and reliability of investment casting for pieces with intricate shape also with selective laser melting of metal powders. We also aspired to produce items that are rather difficult with classical production methods.

To evaluate dimensional precision and definition of ornamental details obtained by means of SLM, we used a metal tile with a compact square pavé structure with ajour on the lower surface, and a ring partially built with a compact hexagonal pavé structure with an ajour in the inner part, an additional challenge due the present of curve surface.

Moreover red gold and platinum hollow wedding rings were used to reduce the weight of jewelry for improving wearability for different wall thickness. The effect of inner reinforcing lattice structures produced with the help of two software, namely Materialise (Magics) and Realizer (RDesigner) was investigated.

Experimental procedure:

In this stage of our study, articles constructions was carried out with a SLM 50 machine (Realizer) equipped with a 100 W power fiber laser having a 10 µm spot, and with a circular 70 mm diameter build platform, placed in a chamber under an argon protective atmosphere.

The alloy powders were produced with a gas atomizer, working in an environment fully protected with argon at atmospheric pressure. This atomizer guarantees the production of a dry powder with a prevalence of spherical particles. These conditions are very important to obtain a good powder flowability under the action of the wiper blade distributing the powder on the build platform. The evaluation of powder flowability was carried out with a Hall Flowmeter Funnel (ASTM B213-03) and with a Carney Flowmeter Funnel (ASTM B964). Apparent density was measured with a standard volume cup (ASTM B212, B329 and B417).

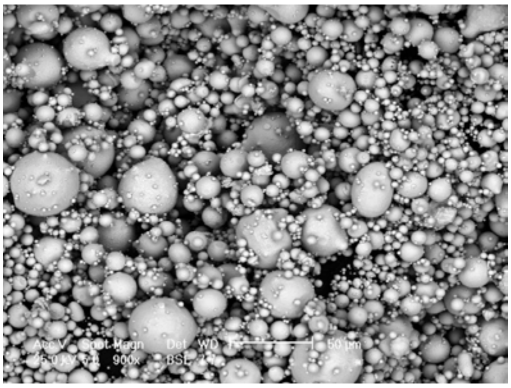

Fig. 1. 750‰ gold alloy powder

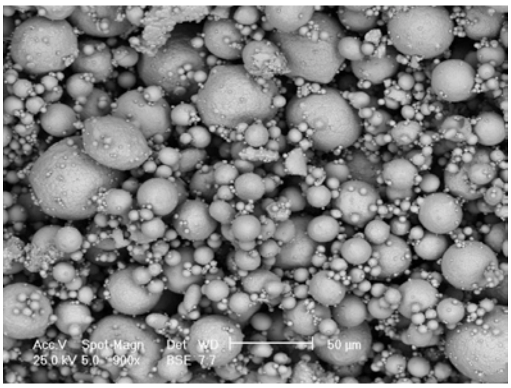

Fig. 2. 950‰ platinum alloy powder

This work can be considered as a natural development of the preceding study [1], because the gold alloy powder contains a semiconductor element different from germanium and was used for the production of plausibly real jewelry items.

The first alloy (alloy 1) was a 750‰ red gold containing silicon with the same atomic percentage of germanium in the previous alloy. Electrical resistivity of silicon is higher than the resistivity of germanium and should ensure a higher absorption of laser radiation. The same atomic percentages of germanium and silicon were used, to have a meaningful comparison of the behavior of the alloys under laser radiation.

The second alloy (alloy 2) was 950‰ platinum with alloying additions slightly different from the cobalt containing alloy used in the preceding work, to be more consistent with the market requirements. The platinum alloy is nearly pure platinum, that absorbs laser radiation effectively, so it was not doped with semiconductor elements.

Both alloys were subjected to SLM with suitable laser parameters, as determined in preceding research.

The shape of powder particles (Figures 1 and 2) was observed with a scanning electron

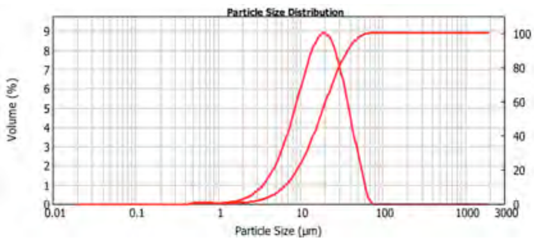

Fig. 3. Particle size distribution in the 750‰ gold alloy powder

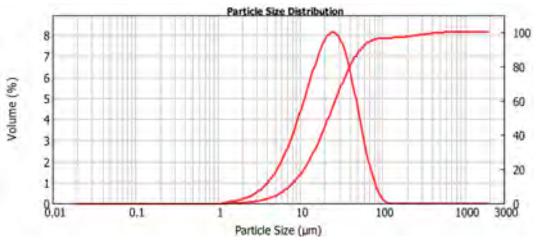

Fig. 4. Particle size distribution in the 950‰ platinum alloy powder

microscope (SEM – EDS) and particle size distribution was evaluated with a Malvern Laser Granulometer Hydro 2000S (Figures 3 and 4). The actual particle size distribution was obtained by removing the larger particles with a Giuliani sieve with a 53 micrometers square mesh. The smallest particles were left in the powder, even though they appreciably reduced the flowability under the (screed) wiper of the build platform (Table 1), because they enable to obtain higher density (i.e. lower porosity) in the produced pieces, as observed in previous studies [2, 3, 4].

ALLOY	Grain Size range (µm)	d_{50} (µm)	d_{90} (µm)	Flowability Hall Flowmeter (s/50 g)	Flowability Carney Flowmeter (s/50 g)	Apparent Density (g/cm³)
1	0-53	17.33	38.12	Non scorre	5.7	8.70 ± 0.05
2	0-53	22.29	54.85	15.2	2.2	11.5 ± 0.05

Tab. 1. Flowability, particle size range and apparent density as a function of particle size distribution

d_{50} = maximum particle diameter in 50 % of the powder volume
d_{90} = maximum particle diameter in 90 % of the powder volume

In this case too the flowability tests showed that flowability of the gold alloy powder is appreciably lower than for platinum powder. This characteristic can be principally linked to the higher content of fine particles in the gold alloy powder.

The evaluation of quality level in SLM pieces was carried out on jewelry pieces stylistically very similar to real ornaments. These were embellished with volumes and artistic details typical of goldsmithing, but without forgetting the rationality and good quality of the building operations.

Therefore the selected objects were adorned with some of the most common decorations present in classic jewelry. These are pavé settings with beads arrangement for stone securing and an ajour on the opposite face. But this set of artistic decorations was simplified and made more symmetric, to allow an evaluation of building accuracy.

The potential of SLM for building an item with multiple stone setting should allow an appreciable time reduction for drilling and cutting the alloy. These operations are usually carried out by the stone setter goldsmith. Only a slight manual revival

Progold S.p.A. progold.com +39 (0445) 492600 info@progold.com

of the alloy should be required before pressing the beads on the stones.

Moreover this study was carried out with alloy powders, that allow an enhanced absorption of laser radiation, to obtain articles with lower porosity and lower surface roughness. This feature was due to the presence of a high number of decoration details, requiring the lowest possible amount of finishing to maintain a high definition and a good dimensional accuracy. This should also enable to reduce the overall presence of defects in a precious alloy. Lastly, an increased absorption of laser energy by the alloy powder enables to operate with a lower radiation power, that means an increased average life of the laser source.

The building performance of SLM was evaluated through the production of a drilled flat square tile with about fifteen millimeters side and one and half millimeters thick (Figure 5). This tile could be a decoration module for producing a wide items set, e.g. pendants, bangles or earrings, just by changing only the fixing system. The tile is endowed with a compact set of sixty one stone seats, each with a diameter of 1.50 mm and oriented along a diagonal, that is according to the highest density of setting.

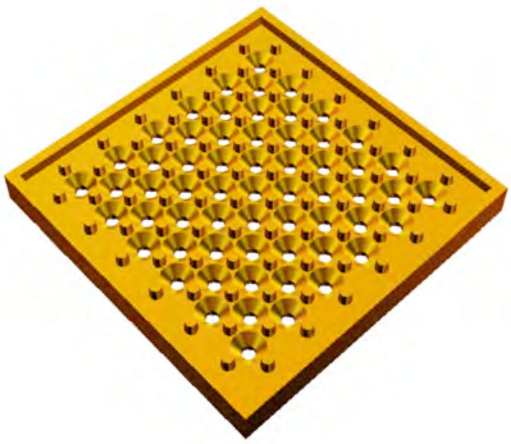

Fig.5. Overall view of the tile with pavé setting

The stone seats are positioned according to a square compact geometry to facilitate the observation of ornamental details during the metallographic examination. The center hole already shows the countersink required to seat the stones. The countersink angle was selected equal to the angle between the girdle plane and the pavilion of the stone, as indicated by the standard parameters of the Tolkowsky cut (40.75°) for diamonds, to reproduce a real manufacturing project with ligthful gemstones and reduced weight.

Fig. 6. Metallographic cross section for quality level evaluation

The beads for setting have truncated cone shape wit 0.50 mm height from the plane of the platelet, base diameter of 0.60 mm and top diameter of 0.50 mm (Figure 6).

The diameter of the through holes of the tile is 0.60 mm, The cutting of the metal in the lower part of the tile, that forms the ajour for the stones, is a part of the decoration suitable for increasing stone brightness. It reduces also the weight of the jewels

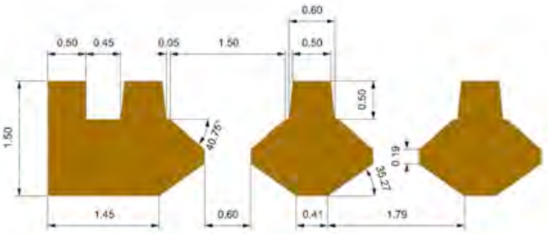

Fig. 7. Detail of the dimensions for quality control

and lead the reduction of precious alloy use. This cut angle is 45°, and avoids the necessity of building supports, reducing the flaws in this part of the specimens. Also the shape interference caused by the alloy residues remaining after recovering the pieces from the build platform is reduced. The value of the cut angle appears to be lower (35.27°) because the shown angle results from the intersection of two ajour planes with the stated 45° slope angle. This fact becomes evident in the cross section parallel to the sides of the tile (Figure 7).

The effectiveness of the process for building the tile prepared for stone setting was evaluated through the comparison of the metallographic cross sections in the directions parallel and transverse to the sides of the specimen (Figure 6) with the corresponding virtual cross sections obtained from the software project.

Different production processes (Pm) were considered for quality evaluation. These are SLM for gold (P1) and platinum (P2) alloys as produced and after a finishing sandblasting treatment (P3, P4) and investment casting of the same articles (P5, P6) without finishing treatments.

PROCESS	L_1	L_2	L_n	l_1	l_2	l_n	$\Delta L_1\%$	$\Delta L_2\%$	$\Delta L_n\%$
P_1	A_1	A_2	A_n	a_1	a_2	a_n	$\Delta A_1\%$	$\Delta A_2\%$	$\Delta A_n\%$
P_2	B_1	B_2	B_n	b_1	b_2	b_n	$\Delta B_1\%$	$\Delta B_2\%$	$\Delta B_n\%$
P_3	C_1	C_2	C_n	c_1	c_2	c_n	$\Delta C_1\%$	$\Delta C_2\%$	$\Delta C_n\%$
P_4	D_1	D_2	D_n	d_1	d_2	d_n	$\Delta D_1\%$	$\Delta D_2\%$	$\Delta D_n\%$
P_5	E_1	E_2	E_n	e_1	e_2	e_n	$\Delta E_1\%$	$\Delta E_2\%$	$\Delta E_n\%$
P_m	F_1	F_2	F_n	f_1	f_2	f_n	$\Delta F_1\%$	$\Delta F_2\%$	$\Delta F_n\%$

Tab. 2. Percent variation $\Delta L_n\%$ of the dimensions as a function of the production process P_m

Dimensional variations for each production process (Pm) of the tiles were determined from the measurement of n nominal dimensions Ln compared with the same real dimensions ln that are considered important for the evaluation of quality level (Equation 1). The values A1, A2, An are the designed characteristic dimensions of the items, while a1, a2, an are the real dimensions measured on them.

Nominal characteristic dimensions Ln were

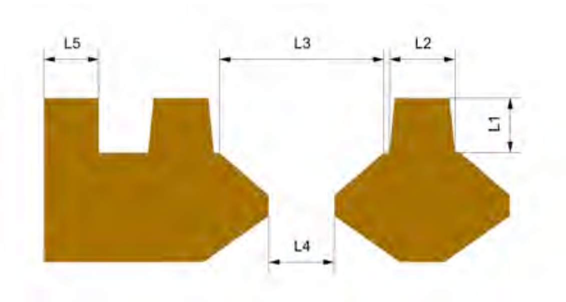

Fig. 8. Metallographic cross section with the indication of the considered dimensions

selected among the most representative ones to analyze the geometry changes of the pieces in the production process as accurately as possible (Table 3).

These values of dimensions were obtained from metallographic cross sections or from stereographic images, depending on the better reliability of the measurements. The reported values are the averages of five measurements (Figure 8).

SYMBOL	DESCRIPTION OF THE DIMENSION
L_1	*Height of the setting beads*
L_2	*Diameter of the beads base*
L_3	*Diameter of the girdle*
L_4	*Diameter of the ajour hole*
L_5	*Rim width of the platelet*

Tab. 3. List of characteristic dimensions for the evaluation of quality level

$$\Delta L_n\% = \frac{|L_n - l_n|}{L_n} \cdot 100 \qquad \text{(equation 1)}$$

Percent variations of each dimension ΔLn% were grouped in intervals to enabling the calculation the combined quality level of the items (Table 4). Each interval corresponds to a specific score si, from one to ten. The lowest score goes to percent variations of the dimensions larger than 35% respect to the nominal value. The highest score goes to percent variations lower than 2%.

The scores *si* obtained from each percent variation of the dimensions ΔLn% are added together to give an overall score Sm. This score was conventionally taken as a quantitative indication of the overall geometrical stability of the items (Equation 2) for a given production process Pm.

$$S_m = \sum_{i=1}^{n} s_i \qquad \text{(equation 2)}$$

Fig. 9. Overall view of the ring with half pavé setting

Fig. 10. Metallographic cross section for quality level evaluation

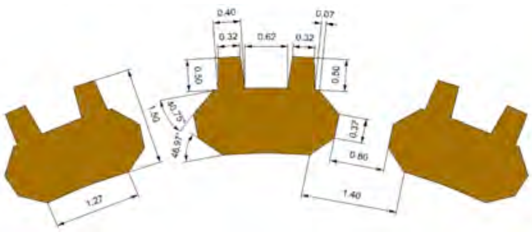

Fig. 11. General and essential dimensions (in red) for quality level evaluation

$\Delta L_n\%$	SCORE (s_i)
35 - 30	1.0
30 - 25	2.0
25 - 20	3.0
20 - 15	4.0
15 - 10	5.0
10 - 8	6.0
8 - 6	7.0
6 - 4	8.0
4 - 2	9.0
2 - 0	10.0

Tab. 4. Score as a function of the range of percent variation of the dimensions

The second part of the evaluation of dimensional accuracy presents a higher level of difficulty, because the pavé decoration is no more onto a plane, but on the curved surface of a ring.

The selected specimen was a ring with pavé settings on half circumference (Figures 9, 10 and 11).

As in the simpler case of the pavé tile, also for the ring dimensional variations of the same characteristic nominal dimensions (Ln) were measured.

The building operation for the pavé ring was carried out with four different orientations of the specimen on the build platform, to verify if there is an optimum orientation, that gives a better quality level. The ring was built vertically with the pavé on the upper side. The orientations concern the rotation of the main axis of the ring with angles of 0°, 45°, -45° and 90°, with respect to the build platform (Figure 12). The effect of the rotation angle can come from the different sweeping angle of the blade distributing the alloy powder respect to the direction of the surfaces of the specimens and from the length variation of the vectors during the building of the layers by the machine.

The following production processes were considered for evaluating the quality level of the ring. SLM with the best (R1) and the worst (R2) orientation on the build table for both the gold and the platinum (R3, R4) alloys, and direct investment casting for the gold (R5) and the platinum (R6) alloy.

The shape of the ring enabled us to improve the quality level evaluation by adding the measurement of surface roughness in parallel and transverse directions respect to the vertical build axis (Figure 13). This characteristic was difficult to evaluate for the pavé platelet, because of his small thickness. Roughness evaluation was carried out with a Taylor Hobson profilometer (Form Talysurf Intra2) equipped with a carbon feeler pin with a 2.0 µm radius diamond tip.

Roughness evaluation enables to create a table with relative scores (rm) (Table 5). These scores, when added to the scores coming from the percent variations of dimensions (Sm), give a total score Stot, that represents a quantitative information on the definition of the items (Equation 3) obtained with a given production process (Pm).

The overall score of roughness is the arithmetic mean of the scores in the vertical and horizontal build direction. In the case of the tile rm is nil.

$$S_{tot} = S_m + r_m \qquad \text{(equation 3)}$$

R_t (µm)	SCORE (r_m)
200 - 300	1.0
150 - 200	2.0
100 - 150	3.0
80 - 100	4.0
60 - 80	5.0
40 - 60	6.0
20 – 40	7.0
10 – 20	8.0
2 – 10	9.0
2 – 0	10.0

Tab. 5. Score as a function of total roughness

In addition to the quantitative evaluation of a set of characteristic dimensional deviations, some more qualitative parameters were selected to establish the accuracy level of the items respect to the ideal design. The selected qualitative parameters mainly concern coherence, definition and symmetry of ornamental details of the pieces in

Fig. 12. Four orientations of the ring on the build platform

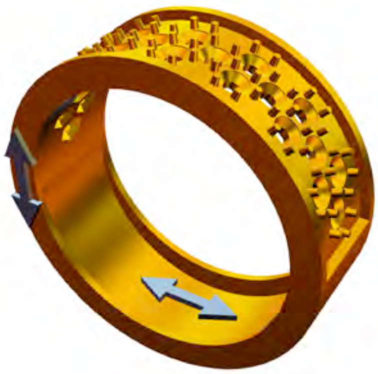

Fig. 13. Places and directions for roughness evaluation on the ring

their global aspect i.e. not localized in a cross section, that represents the jewelry item partially. Each parameter received a numeric score, stating the quality level with figures going from one to ten. The highest score was given only to the virtual object as defined by the software. In this last case alloy porosity and dimensional deviations are nil.

The overall quality index Q(Pm) for each production process was obtained from the product between the total score Stot for the quantitative dimensional deviations and the qualitative index qm for the aesthetic aberration of the specimens (Equation 4).

$$Q(P_m) = S_{tot} \cdot q_m \qquad \text{(equation 4)}$$

The aesthetic aberration quality index qm is obtained from the product of the various scores A1, A2,…,An given to each quality parameter Vi, for the different production processes Pm of the items (Table 6). The product was chosen instead of the summation, because in this way we obtained a more evident difference as a function of the scores related to each quality parameter. So we had a more selective evaluation for the items that can pass the quality control and be accepted for finishing.

The need of having a larger difference in the aesthetic aberration indexes (qm) arises because they come from a subjective evaluation. So it is difficult to define subtle differences among the pieces, that is not the case for the total quantitative score (Stot). Therefore equal scores could be more frequent and hinder useful distinctions.

PROCESS	V_1	V_2	V_3	V_4	V_n	**ABERRATION INDEX (q_m)**
P_1	A_1	A_2	A_3	A_4	A_n	$q_1 = A_1 \cdot A_2 \cdot A_3 \cdot \ldots \cdot A_n$
P_2	B_1	B_2	B_3	B_4	B_n	$q_2 = B_1 \cdot B_2 \cdot B_3 \cdot \ldots \cdot B_n$
P_3	C_1	C_2	C_3	C_4	C_n	$q_3 = C_1 \cdot C_2 \cdot C_3 \cdot \ldots \cdot C_n$
P_4	D_1	D_2	D_3	D_4	D_n	$q_4 = D_1 \cdot D_2 \cdot D_3 \cdot \ldots \cdot D_n$
P_m	E_1	E_2	E_3	E_4	E_n	$q_5 = E_1 \cdot E_2 \cdot E_3 \cdot \ldots \cdot E_n$

Tab. 6. Aesthetic aberration index qm as a function of the quality evaluations Vi

The categories of quality evaluation parameters Vi are essentially related to: symmetry of the setting beads around the stone seats, their general definition in the whole pavé, overall aspect of the taper of the seats, coherence of the ajour cut of the stones and consistence of the alloy rim that forms the boundary of the pavé (Table 7).

We adopted a set of qualitative parameters in addition to the quantitative ones. Even if relatively subjective, they were necessary to get a more exhaustive evaluation of the quality of the built pieces, in comparison with the evaluation that could be obtained from a set of observations on a metallographic cross section. It should never be forgotten that visual appreciation is a crucial and frequently final step of quality control in the factory, to approve the items to be put on sale.

QUALITY INDEX	DESCRIPTION
V_1	Symmetry of the beads
V_2	General definition of the beads
V_3	Overall aspect of the taper
V_4	Coherence of the ajour
V_5	Consistence of the alloy rim

Tab. 7. Categories and description of quality indexes

$Q(P_m)$	DESCRIPTIVE RANK
6000000-4000000	Excellent
4000000-2000000	Optimum
2000000-1000000	Good
1000000-500000	Passable
500000-0	Discarded

Tab. 8. Descriptive rank as a function of overall quality index $Q(P_m)$

The quality level comparison between the precious alloy pieces produced with SLM and direct investment casting was carried out on tile and pavé rings. The investment cast pieces were obtained from models built with a resin whose behavior was similar to a traditional wax injected in rubber molds. This resin was preferred to common acrylic resins for rapid prototyping, because it shows a better definite melting point and leaves a negligible amount of residues in the investment mold. So the formation of many defects is avoided, that could hinder a comparison with traditional waxes.

The resin models were built with a prototyping equipment 3D System CPX 3500 plus with wax jet. In our case is the resin was VisiJet M3 Hi-Cast. The machine procedure was selected in accordance with the best prototyping conditions typically used by the supplier for its own production.

In the case of the gold alloy the same composition of the powder for SLM was not used for investment casting, because the high silicon content could impair the integrity of the pieces. Therefore we selected the alloy showing the highest quality level in our production i.e. GENIA172 (752‰).

The formation of the precious alloy (gold + alloying elements) was carried out through a pre-melting and homogenizing operation in an open furnace under an argon protective atmosphere (5 l/min) at 1100°C. The subsequent investment casting was carried out in a vacuum/pressure machine Indutherm VC480 V at 1020°C.

The red gold trees had two levels with five pieces on each level.

In the case of the pavé pieces, the tiles, having a higher number of stones, were put on the top of the tree to improve filling (Figure 14).

Fig. 14. Rendering of the tree with rings and the pavé tiles

Investment casting of the platinum alloy was carried out with the same alloy used for SLM. In addition to pavé pieces, also classic wedding rings and tensile test pieces were put in the tree, to carry out subsequent comparison tests for mechanical strength. These castings were produced out of our factory by the resin supplier, using an alloy that was previously homogenized in our factory. The investment PRO-TH PLATINUM was used and the alloy was cast at 1770°C in a Yasui VCC centrifugal machine. Preparation of the wax patterns for direct investment casting and casting of the platinum alloy were carried out by the resin supplier Stilnovo S.r.l. of Valenza.

The quality level of the pieces produced through SLM was evaluated considering mechanical characteristics and economic aspects. We evaluated also the possibility of increasing the ductility of SLM pieces, that are usually more brittle than investment cast pieces. Also the weight of ornamental details should be reduced as much as possible, while keeping volume and aesthetic characteristics unchanged. In the same time mechanical resistance and shape stability should be considered.

The pieces produced through SLM are usually harder and less deformable than the same investment cast pieces, because in the building operation the conditions for hardening are present. Moreover microscopic structure defects can be created, that reduce mechanical strength and cold deformability of the alloy. On the basis of production requirements, these characteristics can be modified through annealing treatments, that were evaluated during this study.

Mechanical characteristics were determined through tensile tests in an universal INSTRON dynamometer with a 2kN load cell.

The tensile test pieces have the classic shape of a dog bone with 25.90 mm length, usable length 15.77 mm and 157.73 mm3 volume.

This kind of geometry was selected after a set of tests on test pieces with different geometry (Figure 15).

Fig. 15. Tensile test specimen with dimensions

Tensile test items were produced with SLM and with direct investment casting to evaluate differences in mechanical properties.

The possibility of reducing the weight of jewelry to improve wearability with the same volume and appearance was studied on a classic wedding ring, that was subjected to different levels of hollowing. This operation was possible because of the peculiar way of items construction through SLM. These results cannot be obtained with investment casting (Figure 16). The considered wedding ring has inner diameter of 16.00 mm and outer diameter of 21.00 mm. The width is 5.00 mm and the radius of the semicircular section is 2.50 mm.

Fig. 16. *Complete wedding ring and cross sections of hollowing with dimensions*

Hollowing a solid object such as a wedding ring involves a reduction of the resistance to deformation, therefore the possibility was also

Fig. 17. *Inner structure with square mesh M2 produced with the Magics software (Materialise)*

Fig. 18. *Octahedrical inner structure R2 produced with the RDesigner software (Realizer)*

considered of strengthening the ring by inserting suitable lattice structures in the inner cavity.

Different kinds of metallic internal structures were introduced in the cavities to increase mechanical strength and to modulate wearability and weight of the ring (Table 9).

The first kind of structure consists of a tridimensional framework with square geometry (Mx) obtained with the Materialise Magics 18.02 software. The second kind had octahedrical geometry (Rx) obtained with the Realizer RDesigner 0.6 software.

These types of structure were tested with two density levels, i.e. with a finer texture (R1 and M1) having a 0.5 mm mesh and a coarser texture (R2 and M2) having a 1.0 mm mesh (Figures 17 and 18).

The first level of hollowing, without inner structure, gives a hollow ring with a constant wall thickness of 0.75 mm, with a presumptive mass about 25.7% lower than the solid ring. The second and third level of hollowing give a much more important presumptive mass reduction, i.e. 45.4% and 69.8% respectively.

ID	Wall thickness (mm)	Inner structure type
1	2.5	solid
2	0.75	hollow
3		R_1
4		R_2
5		M_1
6		M_2
7	0.5	hollow
8		R_1
9		R_2
10		M_1
11		M_2
12	0.25	hollow
13		R_1
14		R_2
15		M_1
16		M_2

Tab. 9. List of the amounts of hollowing and inner structure type for the wedding ring

The solid wedding rings made of 950 ‰ platinum, obtained with SLM or with direct investment casting, were subjected to a plastic deformation test, to verify the effect of the production process on mechanical strength and deformability of the alloy. The test was performed with a manual device for enlarging the rings and the increase of the inner diameter to rupture was measured.

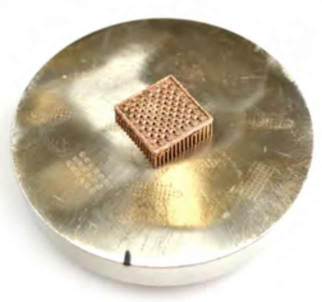

Fig. 19. 750‰ silicon doped red gold pavé tile on the build platform

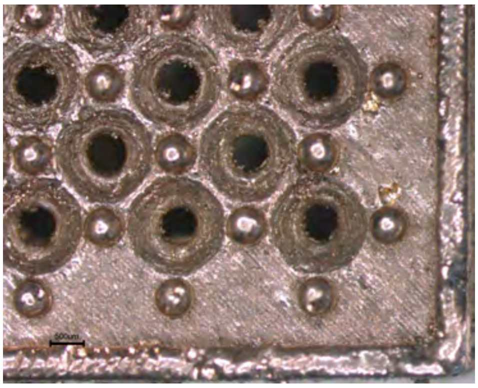

Fig. 20. 750‰ silicon doped red gold pavé tile under the stereoscopic microscope (20x)

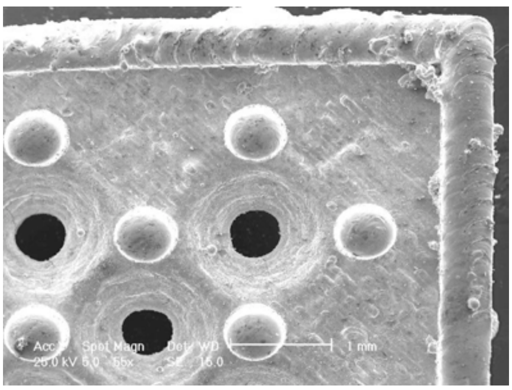

Fig. 21. SEM micrograph of the 750‰ silicon doped red gold pavé tile

Experimental results and discussion:

Optical and scanning electron microscopy evidenced relevant characteristics of the items produced by means of selective laser melting (SLM) as compared with the same items produced by direct investment casting.

In general, the items obtained by using SLM show a significantly superior surface brightness, mainly in the case of the gold alloy. This feature can be attributed to a lower surface roughness of the specimens produced by selective laser melting. However, betimes the construction of some geometrical details seems to have more accuracy and stability for items produced by direct investment casting. This phenomenon can be observed on the rim of the pavé tiles, for instance (Figures 20, 24, 28 and 31). More important differences were observed between gold (Figure 19) and platinum (Figure 23) items: e.g. surface roughness is more evident for platinum (Figures 24, 25 and 26) and rounding of the rims is more marked for the gold alloy (Figure 20, 21 and 22).

Optical stereography of the upper surface of the pavé tiles (Figure 33) allowed the measurement of the girdle diameter (L3), of the ajour hole diameter (L4) of the stones and of the base diameter of the setting beads (L2).

The metallographic cross section of the pavé tiles (Figure 34) enabled to measure the height of the setting beads (L1) and the width of the rim (L5) of the tile. Variations of the characteristic sizes in comparison with nominal quotes are usually included in a range from 0.0% to 35,2% (Tables 10 and 11), where indicating for SLM = Selective Laser Melting, DIC = Direct Investment Casting and SLM + SB = Selective Laser Melting followed by Sandblasting.

In the case of pavé tiles, the silicon doped red

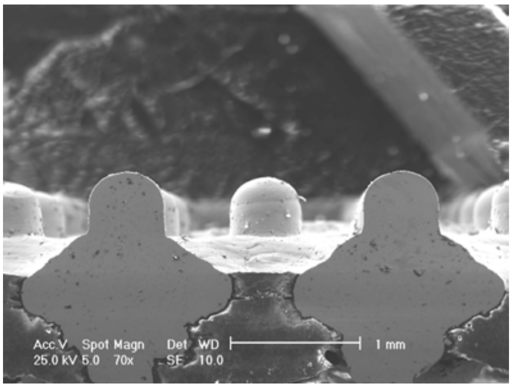

Fig. 22. Cross-sectional SEM micrograph of the 750‰ silicon doped red gold pavé tile

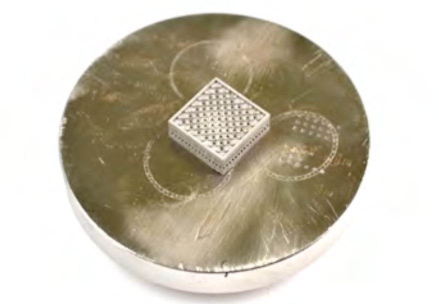

Fig. 23. 950‰ platinum pavé tile produced by SLM

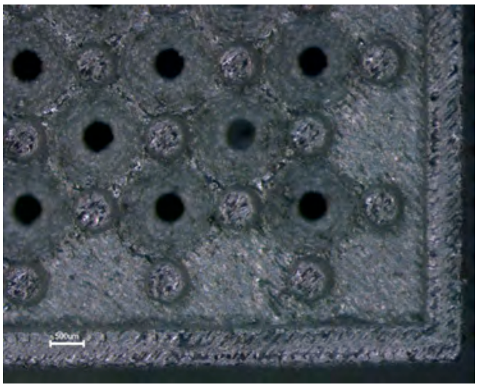

Fig. 24. 950‰ platinum pavé tile under the stereoscopic microscopic (20x)

gold alloy shows a higher conformity with nominal quotes and gets a higher score for the quantitative index Stot when compared with platinum pavé tiles. A similar situation was also observed for the pavé rings. Usually, the items produced by investment casting show a total score for Stot that is lower in the case of pavé tiles, while in the case of the rings only platinum items are better than those produced by using selective laser melting.

PROCESS	L_1	L_2	L_3	L_4	L_5	l_1	l_2	l_3	l_4	l_5	ΔL_1 %	ΔL_2 %	ΔL_3 %	ΔL_4 %	ΔL_5 %	S_t
SLM_{Au}	0.50	0.60	1.50	0.60	0.50	0.51	0.59	1.42	0.61	0.46	2.80	1.33	5.33	1.33	7.20	44.0
SLM_{Pt}	0.50	0.60	1.50	0.60	0.50	0.45	0.58	1.40	0.57	0.56	10.00	3.67	6.93	5.33	12.40	35.0
SLM_{Au} + SB	0.50	0.60	1.50	0.60	0.50	0.50	0.46	1.33	0.54	0.50	0,40	23.67	11.60	10.00	0.00	34.0
SLM_{Pt} + SB	0.50	0.60	1.50	0.60	0.50	0.32	0.45	1.33	0.54	0.56	35.20	25,67	11,60	10,00	12,80	19.0
DIC_{Au}	0.50	0.60	1.50	0.60	0.50	0.47	0.58	1.42	0.54	0.48	6.00	3.33	5.47	9.67	4.00	40.0
DIC_{Pt}	0.50	0.60	1.50	0.60	0.50	0.46	0.53	1.30	0.54	0.52	8.40	11.00	13.47	9.33	3.20	31.0

Tab. 10. Dimension differences as a function of the production process (SLM, DIC, SLM + SB) for the pavé tiles

PROCESS	L_1	L_2	L_3	L_4	L_5	l_1	l_2	l_3	l_4	l_5	ΔL_1 %	ΔL_2 %	ΔL_3 %	ΔL_4 %	ΔL_5 %	S_t
SLM_{Au} 90°	0.50	0.40	1.50	0.80	0.50	0.47	0.45	1.46	0.58	0.52	6.00	12.00	2.67	27.25	3.20	33.0
SLM_{Au} 0°	0.50	0.40	1.50	0.80	0.50	0.48	0.49	1.46	0.61	0.48	3.20	23.50	2.67	24.25	4.80	32.0
SLM_{Pt} 0°	0.50	0.40	1.50	0.80	0.50	0.46	0.45	1.41	0.55	0.60	8.80	13.50	5.87	30.75	19.20	24.0
SLM_{Pt} 90°	0.50	0.40	1.50	0.80	0.50	0.47	0.52	1.43	0.57	0.60	5.20	30.00	4.80	29.00	19.20	24.0
DIC_{Au}	0.50	0.40	1.50	0.80	0.50	0.47	0.37	1.33	0.66	0.49	6.80	8.00	11.60	18.00	2.40	32.0
DIC_{Pt}	0.50	0.40	1.50	0.80	0.50	0.45	0.37	1.41	0.60	0.53	9.60	8.00	6.00	25.00	5.60	32.0

Tab. 11. Dimensions differences as a function of the production process (SLM, DIC) for the pavé rings

In the case of pavé rings, roughness evaluation for gold and platinum alloys showed that in both cases roughness figures on the vertical surface (Figure 27) are clearly lower than roughness figures on the horizontal surface (Table 12 and 13).

Moreover, roughness figures for the gold alloy are generally lower than the average values measured on platinum rings, by about 13 μm in the vertical direction and 23 μm in the horizontal direction.

This observation was also confirmed by the SEM micrographs, evidencing that the surface of platinum specimens are rougher because of the adhesion of a significant amount of fine alloy particles (Figures 25 and 26) during the solidification

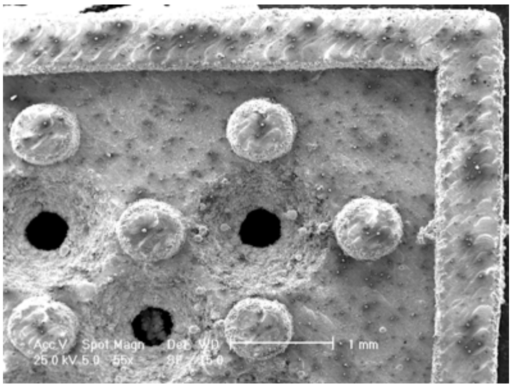

Fig. 25. SEM micrograph of the 950‰ platinum pavé tile

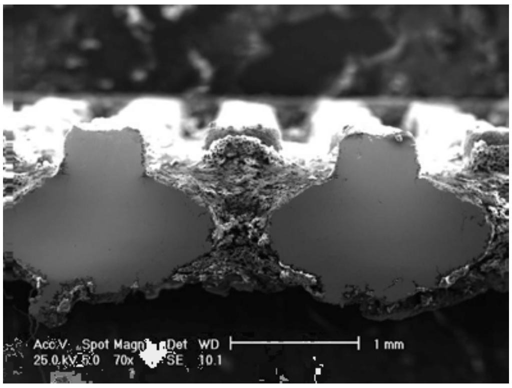

Fig. 26. Cross-sectional SEM micrograph of the 950‰ pavé tile

Fig. 27. 750‰ red gold tree produced by direct investment casting

of the vectors.

Angle (°)	$R_{t\,vertical}$ (µm)	$R_{t\,horizontal}$ (µm)	r_m
0	36,28	60,27	6.0
45	43,64	56,84	6.0
-45	37,96	53,51	6.5
90	26,14	53,19	6.5

Tab. 12. Roughness values and average scores for the gold ring for different orientations

Angle (°)	$R_{t\,vertical}$ (µm)	$R_{t\,horizontal}$ (µm)	r_m
0	41.44	70.53	5.5
45	55.60	85.84	5.0
-45	54.13	76.52	5.5
90	46.08	81.41	5.0

Tab. 13. Roughness values and average scores for the platinum ring for different orientations

The aesthetical aberration index qm, gives a qualitative evaluation of the specimens and decoration details as can be obtained from a visual inspection of the semifinished articles. This index gives a significantly higher score for the pavé tiles produced by using SLM in comparison with the same tiles produced with direct investment casting (Table 14).

The advantage of SLM in comparison with DIC appears to exist for both gold and platinum alloys, but the quality level of the definition for cast items appears to be higher for the red gold. Moreover qm of red gold shows an appreciable increase after sandblasting (SB), mainly because of a quality improvement of the countersink ajour holes and of the rim of the tiles. For platinum, sandblasting appears to scarcely affect the aesthetical aberration index qm.

The situation is quite different for the pavé rings. Firstly, in the case of the best rings the score was inverted in comparison with the pavé tiles, i.e. the silicon doped red gold ring received a score clearly lower than the platinum ring (Table 15). This phenomenon may be ascribed to the different absorption of laser radiation by the platinum alloy. This can allow a better accuracy in the definition of curved surfaces and undercuts.

However the quality index can change significantly, because an influence on the aesthetical aberration index (qm) was observed, depending on the orientation of the specimens on the build platform. This spread can be of some thousands.

The gold rings produced by investment casting show a quality level clearly higher when compared with selective laser melting rings. Investment cast platinum rings show an aesthetical aberration index similar to SLM platinum rings.

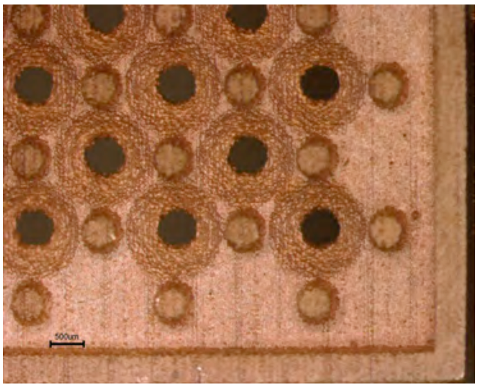

Fig. 28. 750‰ red gold pavé tile produced by direct investment casting (20x)

PROCESS	V_1	V_2	V_3	V_4	V_5	ABERRATION INDEX (q_m)
SLM_{Au}	9.5	8.0	8.5	7.0	7.5	33915
SLM_{Pt}	9.5	7.0	8.5	7.0	7.5	29676
SLM_{Au} + SB	9.5	8.0	9.0	8.5	8.0	46512
SLM_{Pt} + SB	9.5	5.5	9.0	8.0	8.0	30096
MD_{Au}	9.0	7.5	7.0	7.0	7.5	24806
MD_{Pt}	9.5	7.0	6.5	6.5	7.0	19667

Tab. 14. Aesthetic aberration index q_i as a function of the qualitative evaluation V_i for the pavé tiles

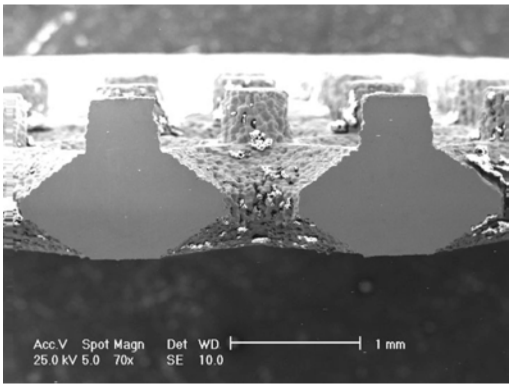

Fig. 29. SEM micrograph of the 750‰ red gold pavé tile produced by direct investment casting

PROCESS	V_1	V_2	V_3	V_4	V_5	ABERRATION INDEX (q_m)
SLM_{Au} (90°)	9.0	8.0	8.0	5.0	7.0	20160
SLM_{Au} (0°)	8.0	8.0	7.0	5.0	7.0	15680
SLM_{Pt} (0°)	9.0	7.0	8.0	6.0	9.0	27216
SLM_{Pt} (90°)	8.5	7.0	7.0	6.0	9.0	22491
MD_{Au}	9.0	7.0	8.5	7.0	8.5	31862
MD_{Pt}	9.0	7.0	7.0	7.5	8.5	28113

Tab. 15. Aesthetic aberration index qi as a function of the qualitative evaluation Vi for the pavé rings

Fig. 30. 950‰ platinum tree produced by direct investment casting

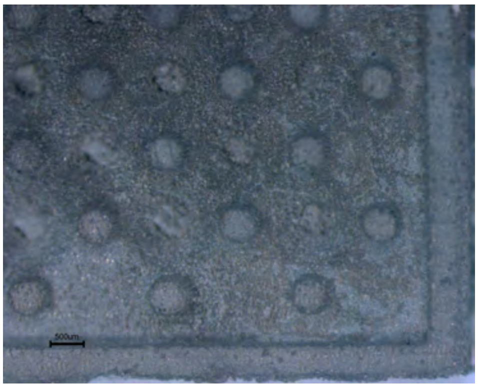

Fig. 31. 950‰ platinum pavé tile produced by direct investment casting (20x)

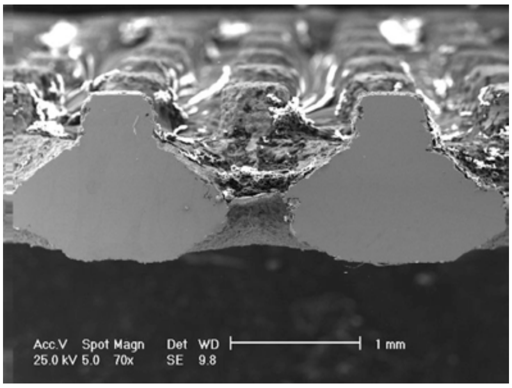

Fig. 32. SEM micrograph of the 950‰ platinum pavé tile produced by direct investment casting

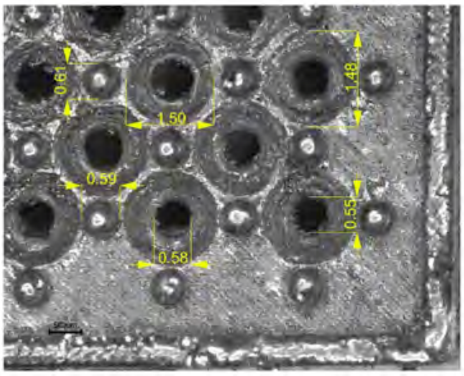

Fig. 33. Set of measurements for the pavé tiles under the stereographic microscope

The sum of the scores obtained from percent variation of quotes (Si) and roughness (rm) gives the total quantitative index (Stot) of the items. The latter, when multiplied for the aesthetical aberration index (qm) gives the overall quality index of the articles Q(Pm).

In the case of pavé tiles, the overall quality index for the red gold pieces is much higher than for platinum items. This happens because the total quantitative score and the aesthetical aberration index are higher for silicon doped red gold items (Tables16 and 17).

Sandblasting improves the visual appearance of the items (qm), but causes the serious problem of lowering quotes accuracy (Stot). On the whole, sandblasting improves the overall quality index for red gold only slightly, but causes a significant dropping for platinum.

Probably, sandblasting has a lower effect on quotes accuracy (Stot) of red gold because of the more aerodynamic shape of the beads (Figures 35 and 36), that lowers the friction into the abrasive particles jet in comparison with platinum beads (Figures 37 and 38).

For both alloys, but mainly for gold, the investment cast pavé tiles show a lower overall quality index when compared with SLM tiles. This happens because the aesthetical aberration factor is lower and the deviation from the nominal quotes is higher (Figure 39).

PROCESS	S_i	r_m	S_{tot}	q_m	$Q(P_m)$	**CATEGORY**
SLM_{Au}	44.0	0.0	44.0	33915	1492260	Good
SLM_{Pt}	35.0	0.0	35.0	29676	1038660	Good
SLM_{Au} + SB	34.0	0.0	34.0	46512	1581408	Good
SLM_{Pt} + SB	19.0	0.0	19.0	30096	571824	Fair
MD_{Au}	40.0	0.0	40.0	24806	992240	Fair

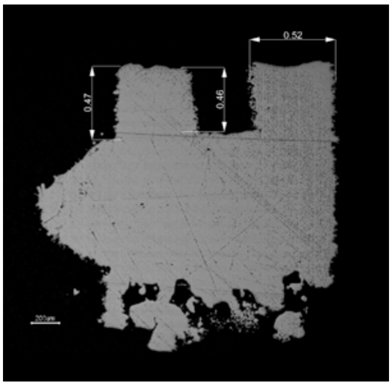

Fig. 34. Set of measurements for the pavé tiles under the metallographic microscope

Fig. 35. Detail of a bead in a red gold pavé tiles before sandblasting

Fig. 36. Detail of a bead in a red gold pavé tiles after sandblasting

MD_{Pt}	31.0	0.0	31.0	19667	609677	Fair

Tab. 16. Averall quality index Q(Pm) for the pavé tiles depending on the production process

PROCESS	S_i	r_m	S_{tot}	q_m	$Q(P_m)$	CATEGORY
SLM_{Au} (90°)	33.0	6.5	39.5	20160	796320	Fair
SLM_{Au} (0°)	32.0	6.0	38.0	15680	595840	Fair
SLM_{Pt} (0°)	24.0	5.5	29.5	27216	802872	Fair
SLM_{Pt} (90°)	24.0	5.0	29.0	22491	652239	Fair
MD_{Au}	32.0	6.0	38.0	31862	1210756	Good
MD_{Pt}	32.0	5.0	37.0	28113	1040181	Good

Tab. 17. Averall quality index $Q(P_m)$ for the pavé rings depending on the production process

In the case of pavé rings the overall quality index shows a another behavior due to different factors. Dimensional accuracy of the best silicon doped gold ring is slightly lower than for the best platinum ring. However in platinum rings the aesthetical aberration index is definitely higher than in gold rings. Therefore the general appearance of the platinum ring is better, as shown by the overall quality index (Table 15). In the items produced with the worst orientation, the difference between gold and platinum alloys is even more relevant (Figure 40).

In any case, the investment cast rings show a better overall quality than the SLM rings. This can be attributed to the easier metal feeding into curved profiles by investment casting. The difficulty of producing wide flat items by investment casting is well known. This difficulty can be overcome by using a properly arranged SLM set up,

The overall quality index for investment cast gold rings is even higher than for platinum rings. This fact comes probably from the better form filling ability and from the lower casting temperature of the gold alloy, respect to the flask temperature

Fig. 37. Detail of a bead in a platinum pavé tiles before sand blasting

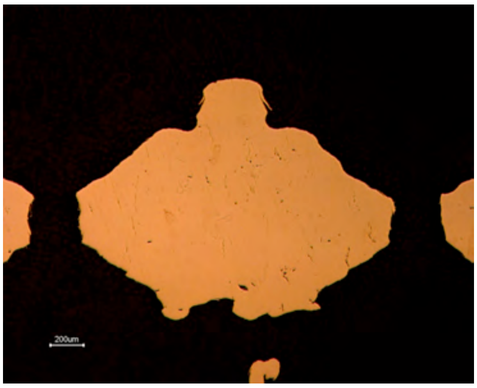

Fig. 38. Detail of a bead in a platinum pavé tiles after sandblasting

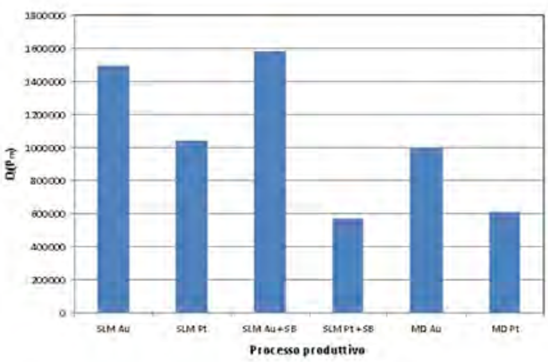

Fig. 39. Overall quality index as a function of production process for the pavé tiles

(Table 15).

The mechanical resistance tests gave interesting information on the behavior of SLM items, those were subsequently subjected to suitable heat treatment. Usually, selective laser melting articles show very good mechanical strength, but can show a low deformation to rupture. This circumstance reduces the possibility of modifying the size of a ring according to the needs of the bearer, for instance. Therefore the possibility was evaluated of increasing ring deformability to avoid early failure. Mechanical tests were performed on silicon doped red gold and platinum alloys dog bone specimens produced by SLM and investment casting as built or subjected to stress relieving heat treatment (Table 18).

In the case of gold alloy, the heat treatment gave a marked increase of ductility, about 34% higher than the value of the unannealed material (εr= 29,4%). On the other hand, for the platinum alloy, the increase of ductility was markedly lower, only 16% of the value for the untreated material. In every case, the ductility of the platinum alloy is lower than the ductility of the gold alloy. The ultimate tensile strength (UTS) was appreciably reduced by the heat treatment. This reduction could also partially be ascribed to a segregation of alloying elements at the grain boundaries, but it requires deeper analysis.

ALLOY	UTS (MPa)	ε_r (%)
SLM_{Au}	455	29,4
SLM_{Au} Annealed	420	39,4
SLM_{Pt}	511	4,11
SLM_{Pt} Annealed	441	4,77

Tab. 18. Ultimate tensile strength and deformation to failure of the alloys as produced or after annealing

Lastly, we studied how to make jewelry articles more purchasable and how to increase their wearability, yet keeping a good mechanical strength. We carried out a process of hollowing on a traditional solid wedding ring, followed by the introduction of inner reinforcing structures. We determined the amount of metal saved by weight measurements with and without inner reinforcing

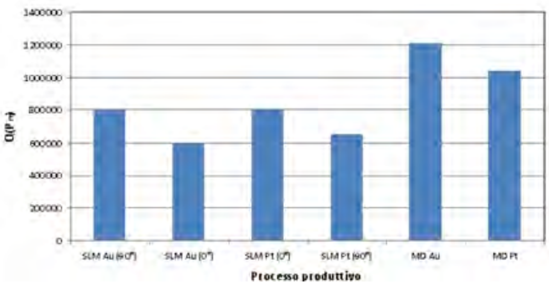

Fig. 40. Overall quality index as a function of the production process for the pavé rings

lattices.

Obviously, the highest weight reduction and precious metal saving was obtained without inner reinforcing structures and it increased with a lower wall thickness of the ring (Table 19). A 0.75 mm thick wall allows a weight reduction of about 25%. With a 0.25 mm thick wall the weight reduction reaches about 63%. This is about the same for both kind of alloys.

The introduction of an inner reinforcing structure causes a reduction of the jewelry economy, but increases the mechanical strength of the ring against the random compression stress.

Ideally, we should reach the maximum level of hollowing, while keeping the highest mechanical resistance to the typical everyday stresses affecting a jewelry piece, such as falling to the floor or compression by the body mass.

Generally, a thinner reinforcing structure (R1, M1) involves a higher density of support material, and corresponding an amount of hollowing lower than in the case of lattices with a larger mesh (R2, M2). However, for the same mesh a square lattice can give a lower level of hollowing when the wall of the ring is very thick (0.75 mm). The amount of hollowing is larger when the ring wall is thin (0.25 mm).

ALLOY	WALL THICKNESS (mm)	REINFORCING LATTICE	WEIGHT AS PRODUCED (g)	WEIGHT REDUCTION (%)
SLM_{Au}	2.50	solid	8.30	0.00
	0.75	none	6.20	25.30
		R_1	7.04	15.18
		R_2	6.28	24.34
		M_1	8.15	1.81
		M_2	6.94	16.39
	0.50	none	4.38	47.23
		R_1	5.15	37.95
		R_2	4.92	40.72
		M_1	8.25	0.60
		M_2	4.98	40.00
	0.25	none	3.10	62.65
		R_1	4.20	49.40
		R_2	3.25	60.84
		M_1	6,80	18.07

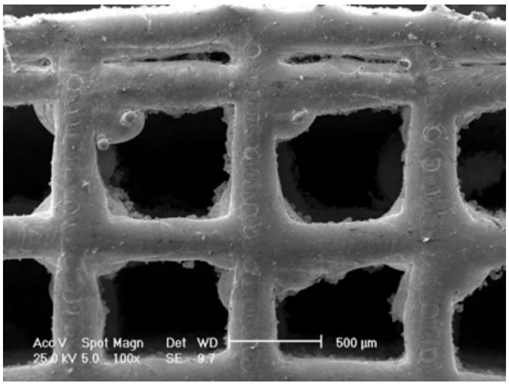

Fig. 41. SEM micrograph of the square support lattice Magics M2

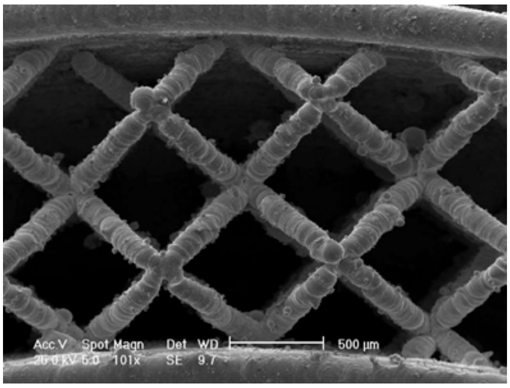

Fig. 42. SEM micrograph of the octahedral support lattice RDesigner R2

Fig. 43. Microstructure of platinum solid ring produced by direct casting

		M_2	3.70	55.42
SLM_{Pt}	2.50	solid	11.31	0.00
	0.75	none	8.66	23.43
		R_1	9.20	18.66
		R_2	8.86	21.66
		M_1	11.05	2.30
		M_2	9.40	16.89
	0.50	none	6.72	40.58
		R_1	7.60	32.80
		R_2	6.80	39.88
		M_1	10.90	3.63
		M_2	7.88	30.33
	0.25	none	4.40	61.10
		R_1	5.46	51.72
		R_2	4.84	57.21
		M_1	8.90	21.31
		M_2	5.74	49.25

Tab. 19. Hollowing modes for wedding rings and related weight variations

This circumstance happens because, in the case of octahedral lattice (R1, R2), the thickness of the support structures is considerably lower, because of the different building procedure of the used software (Figures 41 and 42) even if the mesh is unchanged.

Enlargement test on the platinum wedding rings evidenced a rather surprising phenomenon that apparently disagrees from preceding observations i.e. that the annealing heat treatment should increase the deformability of the alloy. The solid platinum wedding rings produced by using SLM, both as produced and after the annealing treatment (980°C, 25 minutes), do not tolerate any enlargement degree and break immediately as deformation starts. A similar effect was observed for the investment cast platinum rings after annealing. On the contrary, the solid investment cast platinum rings, as recovered from the tree, can tolerate outstanding enlargement degree before failure, i.e. from a starting diameter of 16.00 mm up to about 20.35 mm.

The typical microstructure of platinum solid ring obtained by direct investment casting without annealing reveals quite big dendritical equiaxed grains with an average size of about 300 µm (Figure 43). The grain boundaries are sharpe and they do not seem evidencing segregation that could lead embrittlement. On the other hand, the solid ring produced by selective laser melting showed a much more fine grain sized microstructure of about 30 µm, as a consequence of a rapid cooling of the molten vector. The sudden failure showed by selective laser built items under tensile stress could be maily ascribed to the propagation of intervectorials crevice (Figure 44, 45). In less extent, the mechanical failure can be considered as intergranular. The formation of microcravices requires deeper investigation and probably it depends on imperfect joints consecutive vectors. Fortunately, this flaw does not affect the quality of polished articles.

This phenomenon could be ascribed to the precipitation of embrittlement phases (GaPt3) at the grain boundaries, but also to possible microstructural decay in the case of selective laser melting specimens. As cast platinum rings are rapidly water quenched after centrifugal casting and intermetallic compounds may not have time to segregate, as consequence of high temperature level, but this needs more enquirings.

Lastly, a preliminary setting test was carried out on the beads of the pavé tiles of both alloys typology, to check their securing ability on the stones. This test was carried out to verify the compression resistance of the alloys, that showed low deformability under tensile stress, mainly for platinum. The four beads around a hole were formed with a beading tool of suitable size. Then the shape was observed under the stereoscopic microscope and the shear resistance of beads was evaluated by side pressing with the tip of the beading tools. Interestingly, also the most brittle platinum alloy gave strong setting beads, suitable for securing a stone (Figure 46, 47, 48 and 49).

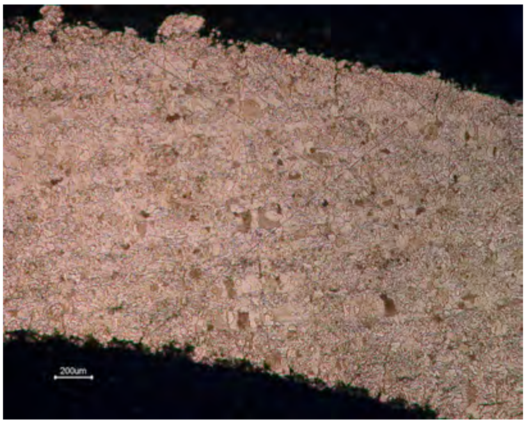

Fig. 44. Microstructure of platinum solid ring produced by selective laser melting

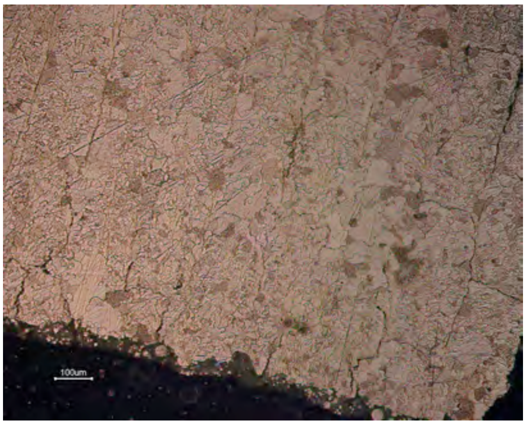

Fig. 45. Detail of the intervectorials failure of platinum solid ring produced by selective laser melting

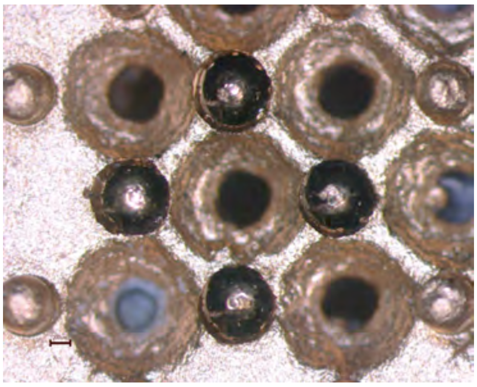

Fig. 46. Forming of the beads on the SLM produced gold pavé tiles

Conclusions:

The general outcomings of last experiments are rather promising, when the quality level of the items produced by SLM is considered. The flat specimens, i.e. pave tiles, show an overall quality level appreciably higher than the specimens with curved profiles. This can be observed by comparing the difference between the overall quality indexes

Fig. 47. Forming of the beads on the SLM produced platinum pavé tiles

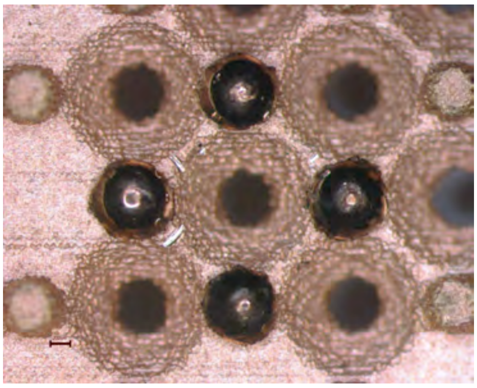

Fig. 48. Forming of the beads on the direct investment cast gold pavé tiles

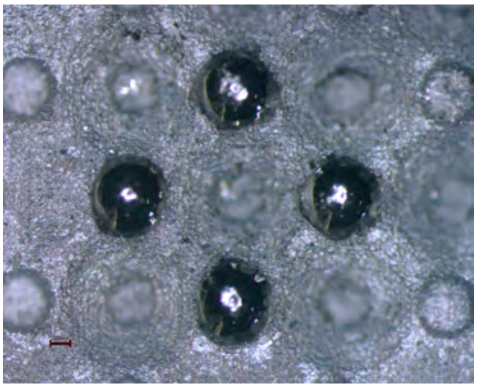

Fig. 49. Forming of the beads on the direct investment cast platinum pavé tiles

Q(Pm) of the pavé tiles with that of the pavé rings, that amounts to some hundreds of thousands. This situation is opposite when the same items are produced by direct investment casting, because the latter process typically suffers with problems in producing flat surfaces.

In the production of the pavé tiles, i.e. the flat items, the silicon doped gold alloy gives an overall quality index clearly higher than platinum. The dimensions are more accurate and the general appearance of decorative details is more consistent with the design.

In the production of rings, the platinum alloy is significantly better for the general consistency of the decorative details but is inferior for quotes accuracy.

In conclusion, the overall quality level of the rings is somewhat similar for both precious alloys. As for mechanical properties, the silicon doped red gold alloy shows higher ductility than platinum. However, for both alloys the securing tests on the setting beads for pavé tiles showed a good resistance to compression and shear stresses that are typically developed during gemstones setting.

References:

SFS Paper

1. D. Zito et al., "Optimization of SLM Technology Main Parameters in the Production of Gold and Platinum Jewelry", *The Santa Fe Symposium on Jewelry Manufacturing Technology 2014*, ed. Eddie Bell (Albuquerque: Met-Chem Research, 2014).
2. D. Zito et al., "Optimisation of the Main Selective Laser Melting Technology Parameters in the Production of Gold Jewellery", *The Santa Fe Symposium on Jewelry Manufacturing Technology 2013*, ed. Eddie Bell (Albuquerque: Met-Chem Research, 2013).
3. D. Zito et al., "Latest developments in Selective Laser Melting production of gold jewellery", *The Santa Fe Symposium on*

Jewelry Manufacturing Technology 2012, ed. Eddie Bell (Albuquerque: Met-Chem Research, 2012).

Journal Article

4. Kruth, J., Mercelis, P., Froyen, L. and Rombouts, M. (2004), "Binding mechanisms in selective laser sintering and selective laser melting", *Proceedings of the Solid Freeform Fabrication Symposium*, pp. 44-59.
5. Yadroitsev et al., "*Factor analysis of selective laser melting process parameters and geometrical characteristics of synthesized single tracks*", Rapid Prototyping Journal, 3(18)(2012)201-208.